NEWLY APPRECIATED ROLES FOR ELECTRONS IN ION-ATOM COLLISIONS

Ivan A. Sellin

Department of Physics and Astronomy
University of Tennessee, Knoxville, TN 37996
and
Oak Ridge National Laboratory, Oak Ridge, TN 37831, USA

Abstract

Since the previous Debrecen workshop on High-Energy Ion-Atom Collisions there have been numerous experiments and substantial theoretical developments in the fields of fast ion-atom and ion-solid collisions concerned with explicating the previously largely underappreciated role of electrons as ionizing and exciting agents in such collisions. Examples to be discussed include the double electron ionization problem in He; transfer ionization by protons in He; double excitation in He; backward scattering of electrons in He; the role of electron-electron interaction in determining beta parameters for ELC; projectile K ionization by target electrons; electron spin exchange in transfer excitation; electron impact ionization in crystal channels; resonant coherent excitation in crystal channels; excitation and dielectronic recombination in crystal channels; resonant transfer and excitation; the similarity of recoil ion spectra observed in coincidence with electron capture vs. electron loss; and new research on ion-atom collisions at relativistic energies.

Introduction

The role of electrons as passive, shielding agents in ion-atom collisions, whose effects are largely taken into account by central field approximations and by Pauli antisymmetrization, has a long and successful history in explicating many fascinating collision phenomena among electrons, ions, atoms, and molecules in general, and ion- atom collisions in particular. The active role of electrons as ionizing and exciting agents in their own right has been generally less well appreciated. In thinking over the various possibilities for responding to Prof. Berényi's injunction to keynote speakers – to give "special emphasis to the development in the recent three years, pointing out the most actual problems of the field and also the future tendencies as you observe them"– it seemed to me that recognition of this active participation of electrons as ionizing and exciting agents in the course of ion-atom collisions has been a distinguishing feature of many of the most stimulating papers that have appeared in the literature of the field during these past three years. Hence the choice of title: the term "Newly Appreciated" emphasizes that the processes to be discussed have always been prominent in the physics – what is new is mainly our improved insights into them.

We will divide our discussion, somewhat arbitrarily, into two parts: the first in which electron-electron and electron-ion interactions are internal to one of the two colliding systems, and the second in which these interactions are shared.

Internal Electron-Electron Ionization And Excitation Interactions

We take as a starting point double ionization by photons, since a single photon projectile interacts cleanly with only one target electron. Double ionization is entirely attributable to electron correlation, taken here to mean Coulomb interaction among target electrons, and to include exchange effects. Even for photoionization, which lacks the complexity of the heavy collision partner, other complexity immediately arises: double ionization can arise from direct ejection of two electrons; or from a two-step process

where photoionization of an inner shell electron is followed by an Auger transition; or by a two-electron Auger decay following creation of an inner shell vacancy.

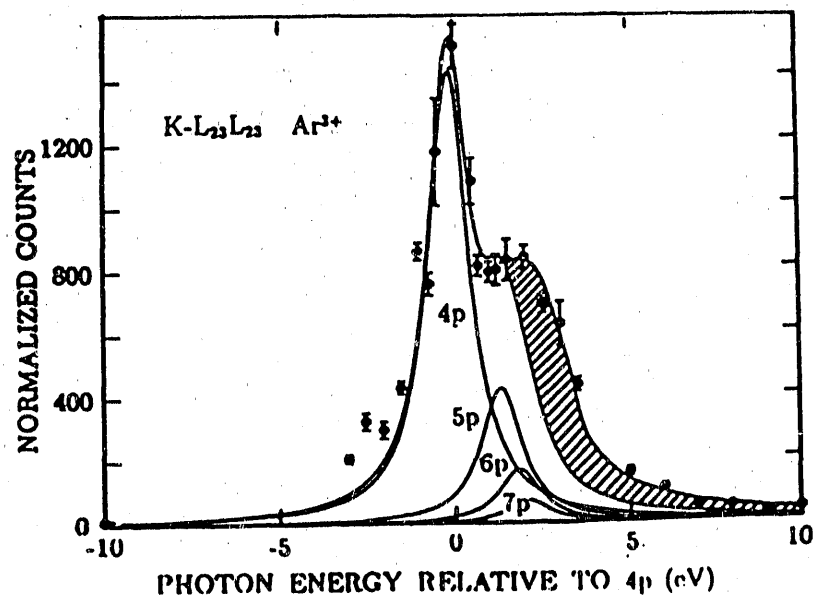

Fig. 1. Decomposition of Ar^{3+} photoion yields observed in coincidence with K-L_{23}-L_{23} autoionization electrons into components resulting from excitation of an Ar K electron into bound *np* levels. The shaded area represents recapture of the photoelectron by post-collision interaction. From J. Levin et al., Ref. 1.

An example of how large internal electron-electron ionization probabilities can be is illustrated by a recent experiment of Levin et al[1], who studied the photoion spectrum resulting from the Auger decay of Ar atoms which had been resonantly photoexcited to the $4p, 5p, 6p, 7p$ .... levels of neutral Ar. Analysis of the photoion spectrum reveals that the L-MM decay of each of the two L_{23} vacancies usually formed in the most probable K-LL autoionization decay channel additionally ionizes ≈27% of these Rydberg electrons, with the ionization probability of $7p$ electrons reaching $\gtrsim$ 55%! Figure 1 illustrates the excitation function of one of the photoion states observed as a function of photon energy. As the exciting photon energy is raised in energy above the Rydberg resonances to just above ionization threshold, a prominent shoulder in the excitation function is seen, exhibiting the interesting phenomenon of recapture of the photoelectron by post-collision interaction with departing Auger electrons, reducing the charge of the residual ion from the expected, above threshold diagram value from +4 to +3.

Two-Electron Ionization in He

In view of the complex as well as highly probable internal electron-electron interaction phenomena accompanying inner-shell excitation phenomena just noted, even for the simple case of photon - single electron interactions, it is natural that the greatest progress in understanding dynamics of both photon and ion interactions with atoms in which electron correlation is important has concerned the simplest such target, He. Even for He, a number of surprises keep turning up.

For example, it is interesting to compare single and double photoionization cross sections with corresponding charged particle interaction cross sections. In the limit of high photon energies and projectile particle energies (say above 10 times the ionization potential and 10 MeV/u, respectively), the naive expectation is that apart from kinematic factors the particle and photoionization cross sections approach converge to the

same values. Because of its specific sensitivity to electron correlation in double ionization, and because common factors drop out, it has become customary to compare R, the ratio of the double to single ionization cross sections in each case rather than the raw cross sections themselves. Yet this ratio is found to lie[2] in the range $R(h\nu) = 4$ to 5%, and R(protons, antiprotons, electrons) in the range 0.2 to 0.4%, more than an order of magnitude different[3-5]. Actually, $R(h\nu)$ is surprisingly ill established experimentally, and is based on scattered data which is remarkably sparse above 200 eV, and could profit from new measurements at higher photon energy[6]. Until the comparatively recent work reported in Refs. 3 - 5, little was firmly established about the asymptotic limit for the charged projectile case as well.

Reading and Ford have attributed the difference in R to the fact that "the ejected electron in a high-energy ion-atom collision moves rather slowly away from the atom. Thus the shakeoff limit is not applicable, and gives a cross section predicted to be an order of magnitude higher than observed..." Here shakeoff refers to the sudden ejection of one electron, leaving the other to collapse from a single-particle orbit in neutral He to an appropriate linear combination of states in He^+, including those shakeoff states lying in the He^{2+} ionization continuum.

The divergent approach to an asymptotic R value common to electrons, positrons, protons and antiprotons at large v_P has a rich experimental and theoretical background much of which almost (but not quite) fits into the three-year span of central interest here. A succinct summary of events has been provided by Heber et al.[5] Following up interesting differences between cross sections for double ionization for equal velocity electrons and protons (cf. Fig. 1, first article, Ref. 6), more recent experiments and theory have successfully sought to compare data for equivelocity protons and antiprotons[3,4] and electrons and positrons[7]. These experiments have shown that the observed differences reflect a large effect associated with projectile charge sign. At projectile velocities corresponding to $\sim$ 1 MeV/u R is found to about be a factor of 2 larger for electrons and antiprotons than it is for positrons and protons. Above 10 MeV/u the R values for all four projectiles appear to level off at about 2 - 3 x 10^{-3}.

A number of interesting possible mechanisms to explain these particle-antiparticle differences were discussed (and some rejected) by Andersen et al.[3] Among these were shakeoff, disregarded for reasons already given; a two-step (second Born approximation) process labelled $TS-1$, in which a first electron "struck" by the incident projectile goes on to knock out a second (scaling as the second power of the projectile charge); another two-step mechanism thought important at lower projectile velocities labelled $TS-2$, consisting of two consecutive projectile-electron encounters in the same collision (scaling as the fourth power of the projectile charge). Since the particle-antiparticle differences reflect an odd power of the charge, two interference effects were considered. Interference between $TS-2$ and shakeoff, or between $TS-1$ and $TS-2$, may account for these differences. In fact, it has recently been shown by Végh and Burgdörfer[3] that $TS-1$ and shakeoff are equivalent (up to a sign).

Subsequently the novel calculations of Reading and Ford, using their so-called forced impulse method, not only produced good qualitative understanding of the magnitude and velocity dependence of R for both protons and antiprotons, but also (with the inclusion of d as well as s and p orbitals in their basis) quantitative agreement with the asymptotic value of R. Figures 2 and 3, drawn respectively from Ref. 4, item 2, and Ref. 5, illustrate these points. The former reference attributes the proton-antiproton difference primarily to an interference between first and second Born amplitudes depending critically on non-dipole transitions, without commenting further on the relative merits of the interference mechanisms identified by Andersen et al. The dotted curve shows the prediction of Ford and Reading multiplied by 1.35. Convergence toward a good understanding of the double ionization problem seemed well on its way until publication of the results of Heber et al., who used beams of N^{7+} ions to study R in the 10 - 30 MeV/u range. In these experiments R was found to remain nearly constant over the

velocity range at about 0.01, some 4 - 5 X higher than the high-velocity limit established previously for $q = 1$ projectiles, and also found for 20 MeV/u He projectiles! On this disquieting note we end this discussion of double ionization in He, and pass on to the closely related subjects of transfer ionization by protons in He, and double excitation of He by fast ions.

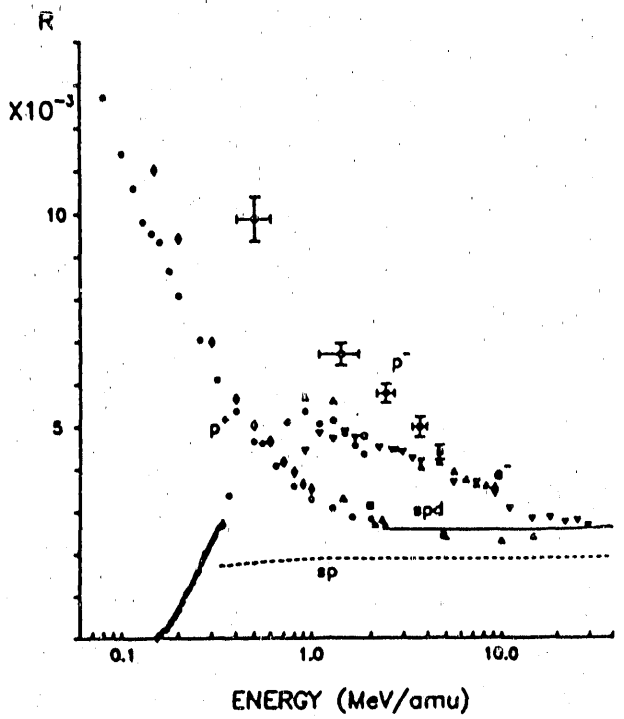

Fig. 2. The ratio R between double and single ionization cross sections for antiprotons, protons, and electrons in He. The broken and full curves labelled *sp* and *spd* are first Born results of Ford and Reading, Ref. 4, item 2. Filled squares, antiproton data from Ref. 3. Other filled symbols, electron data. Open symbols, proton data. References to experimental data are given in Ref. 4, item 2.

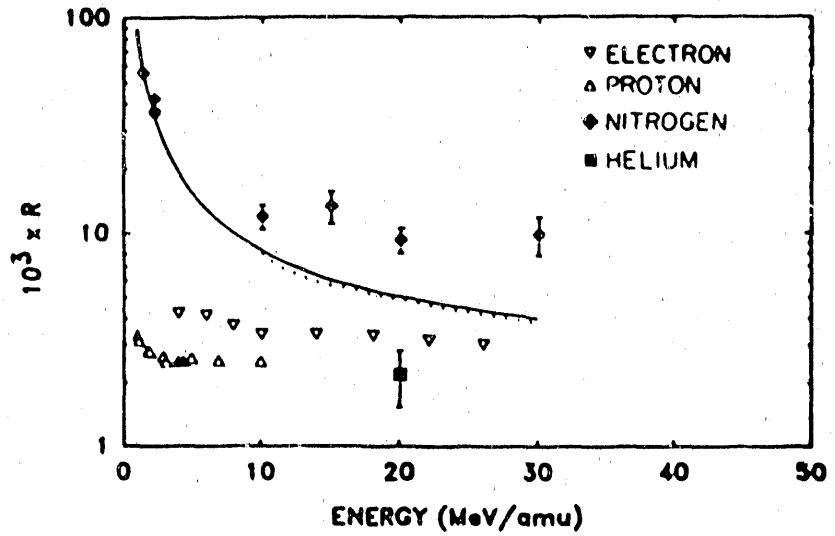

Fig. 3. Comparison of R found by Heber et al. for nitrogen and helium projectiles with other data for electrons, protons, and low- energy nitrogen ions. References to the other data as well as to a semiempirical calculation of H. Knudsen et al. are given in Ref. 5.

Transfer Ionization by Protons in Helium

In a recent experiment Pálinkás[8] et al. investigated the angular distribution of electrons ejected from He near the projectile velocity in coincidence with the capture of the other electron by 1 MeV protons, a special case of double ionization usually referred to as transfer ionization. In an approximate description of the process studied, the captured electron first collides with the proton, and then scatters into a bound state of the projectile through a second collision with the other electron (p-e-e scattering). The signature of the process is a peak near 90° in the angular distribution of the ejected electrons, and is illustrated in Fig. 4. Good agreement for this very small cross section is found with the second Born calculations of Briggs and Taulbjerg.[8]

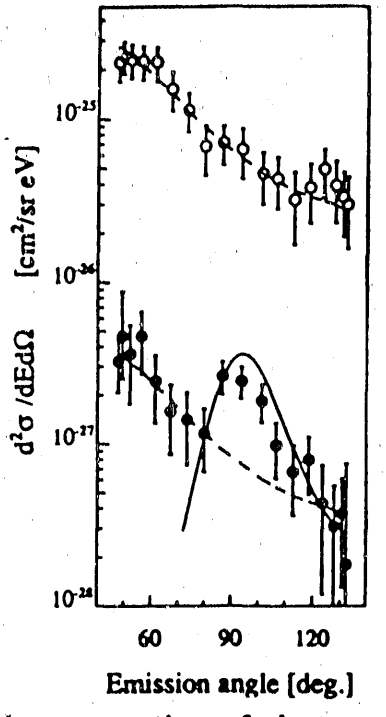

Fig. 4. Doubly differential cross section of electron emission at 600 eV following transfer ionization of Ne (open circles) and He (closed circles) by 1 MeV protons. The solid curve is derived from Briggs and Taulbjerg. From J. Pálinkás et al., and J. Briggs and K. Taulbjerg, Ref. 8.

Double excitation of He by Fast Ions

The kinship of double excitation of He by charged particles to double ionization has been explored recently by J. Giese et al.[9], who note that double excitation leads to better understood states of well defined energies, quantum numbers, and angular distributions, but also the drawback of requiring interpretation of interferences between these resonances and the underlying single ionization continuum. First and second order processes quite analogous to those already discussed for the two-electron ionization problem enter, with corresponding opportunities to study first order processes scaling as the second power of the projectile charge q, second order processes scaling as q^4, and various possible interferences scaling as q^3. Better understanding of these scalings was sought through exploration of the projectile charge q dependence of the electron emission yields from the doubly excited $2s^2(^1S)$, $2s2p(^1P)$, and $2p^2(^1D)$ states of He produced by electrons, protons, C ions (q=4-6), and F ions (q=7-9). The results indicated that excitation to the $2s^2$ and $2p^2(^1D)$ states increase approximately as $\lesssim q^3$, while excitation

to the $2s2p$ state varies as approximately q^2. Figure 5 illustrates the total cross section data obtained for the $2p^2(^1D)$ state scaled by q^2, together with overlapping earlier data of Pedersen and Hvelplund[9], and a very recent coupled states calculation of Fritsch and Lin[9]. The Fritsch and Lin calculation is said to specifically treat electron-electron interactions, and is seen to give a much steeper q dependence than the data.

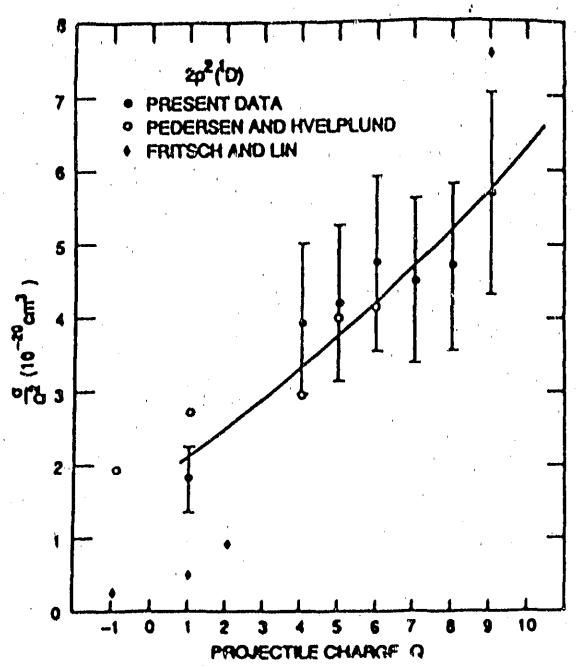

Fig. 5. Total averaged emission cross section for the $2p^2(^1D)$ state scaled by q^2. Open circles represent corrected data of Pedersen and Hvelplund, while the diamonds represent calculations of Fritsch and Lin. From Ref. 9.

Shared Electron-Electron Ionization And Excitation Interactions

We turn now to the some of the many recently observed, highly interesting manifestations of electron-electron and electron-ion interactions in situations where the excitation or ionization of one partner in an ion-atom collision is attributable to collision interactions with the other. The first of these to be considered is backward scattering of electrons from projectile ionizing collisions.

Backscattering of Electrons in Projectile Ionizing Collisions

An exploratory study of projectile ionizing collisions (which includes electron loss to continuum, ELC) for ≈ 0.5 MeV/u He^+ on He, Ne, Ar has been undertaken by Köver et al. of ATOMKI in Debrecen, working together with Heil et al.[10] of the University of Frankfurt. A plot of singly differential cross sections $d\sigma/d\Omega$ vs. electron ejection angle is shown in Fig. 6.

The strong deviation of the measured data from two theoretical calculations, one using plane wave Born approximation by Köver, Szabó, Heil et al, and the second by Hartley and Walters[10], is especially evident at the most backward angles. According to calculations in progress by Wang and Burgdörfer[11], the most likely explanation is the increasing prominence of a second order process involving electron - electron inelastic scattering in combination with a hard elastic scattering of the freed electron with the nucleus.

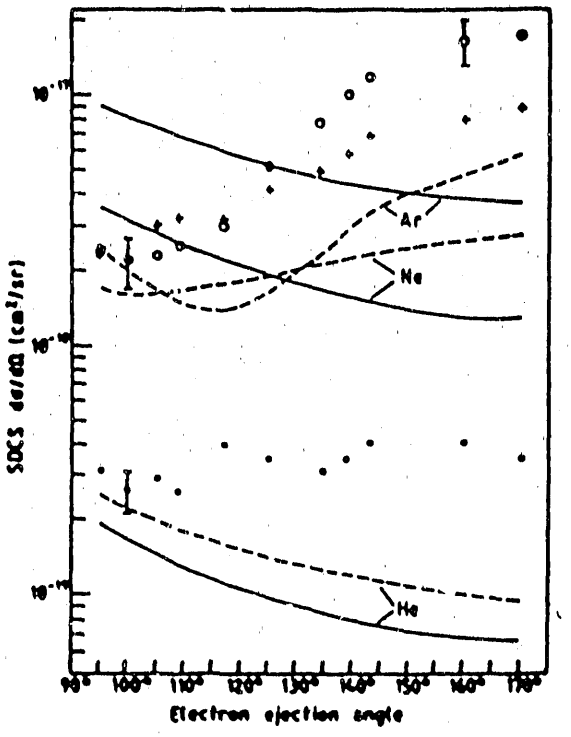

Fig. 6. Singly differential cross section for projectile ionization for 2 MeV He^+ on He, Ne, Ar collisions over the range 90 to 180 deg. From Ref. 10.

Sign Change in Quadrupole Asymmetry Parameter β_2 in He^+ - He ELC Cusps

ELC corresponds to the fraction of projectile ionization electrons emitted within some half-angle of collection Θ_0 of the forward direction. Under some circumstances, e.g. for loss from $He^+(2p_0)$ substates in He^+ - rare gas collisions at sufficiently high velocities for the Born approximation to apply, Burgdörfer et al.[11] found that in the now familiar multipole expansion of the ELC angular distribution, the quadrupole (β_2) component can take on large positive values. For sufficiently large values, a dip or inversion near the tip of the cusp can occur.

For He^+ - He collisions in the range 50 - 150 keV/u, Gulyás et al. find the steep variation of β_2 with beam velocity illustrated in Fig. 7. Since it is a feature of the theory that inelastic electron - electron interactions reduce the value of β_2, its rapid decrease to negative values are thought to reflect a correspondingly speedy onset of the importance of inelastic electron-electron collisions in this ELC process. The decrease observed is considerably more rapid than found in the related theoretical calculations, which are also illustrated in Fig. 7.

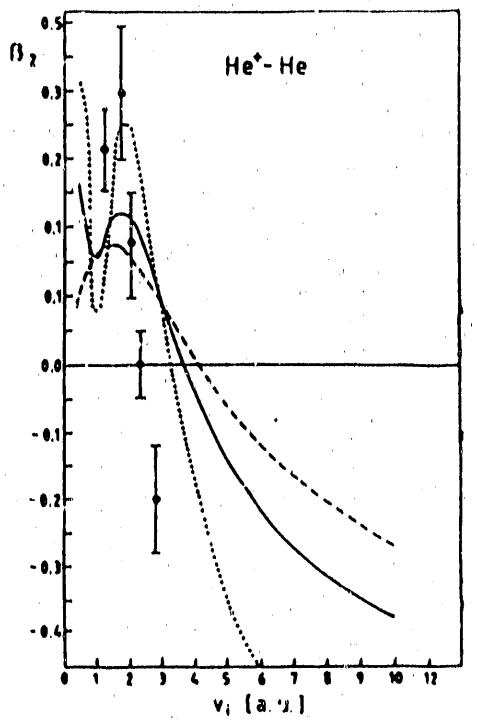

Fig. 7. β_2 parameter for He^+ - He collisions as a function of projectile velocity. Full circles, experiments of Gulyás et al. Theory from Burgdörfer, Szábo et al.: dashed line, initial state of projectile, 1*s*; dotted line, 2*s*; solid line, 80% 1*s* plus 20% 2*s*. From Ref. 11.

Projectile K Ionization by Target Electrons

Very clear illustrations of electron-electron interaction between projectile and target electrons are provided by very recent measurements by Hülskötter et al.[12] of cross sections for projectile K-shell ionization for 0.75 - 3.5 MeV/u C^{5+} and O^{7+} projectiles colliding with H_2 and He targets. Some of the experimental results are displayed in Fig. 8.

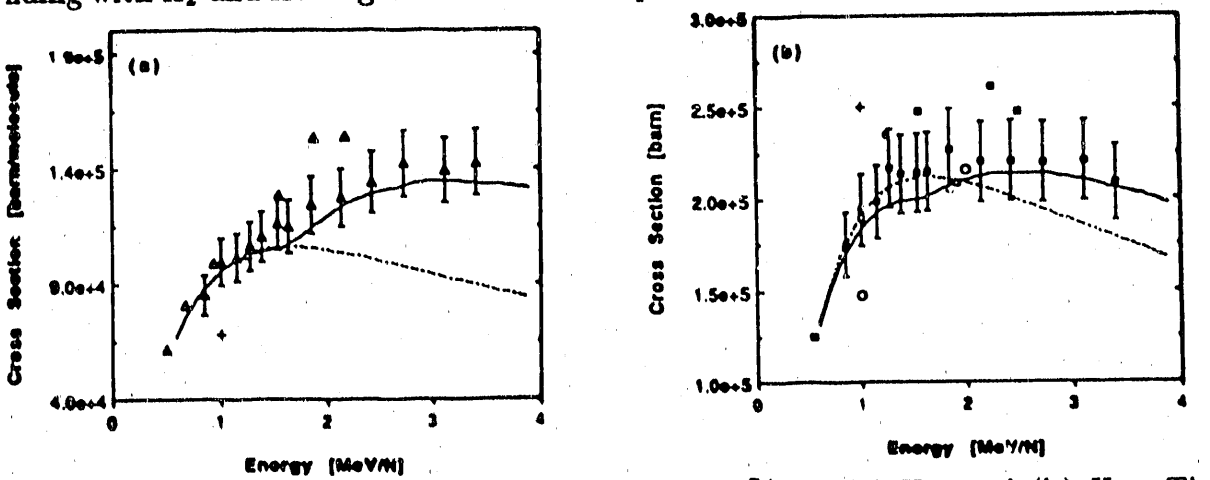

Fig. 8. Projectile ionization cross sections for O^{7+} on (a) H_2, and (b) He. The solid curves give the results of screening-antiscreening calculations described in Ref. 12, and the dashed curves pure PWBA calculations. The solid symbols display the recent experimental results of Hülskötter et al., and the open symbols earlier results from other laboratories (see citations in Ref. 12).

In explaining the observed data, the authors take into account the effect of target electrons by introducing a screened Coulomb interaction between the projectile electron and the target, where however the target electrons not only act coherently as screening agents, but also incoherently as ionizing (antiscreening) agents. The experimental results are found to agree with plane wave Born approximation calculations which take both into account. For energies for which the target electrons have sufficient energy in the projectile frame to ionize the projectile electron, the electron-electron interaction thus leads to a significant observed increase in the total ionization cross section.

Spin Exchange in Transfer Excitation

A direct manifestation of the interaction of projectile and target electrons has been studied by Zouros et al.[13], who measured the production of $1s2s2p\,^4P$ projectile states excited in collisions of $1s^22sO^{5+}$ and F^{6+} with He and H_2. The ^4P state cannot be produced in direct projectile electron - target nucleus excitation, since the necessary electron spin flip is very rare for such low Z ions. However, $1s$ to $2p$ excitation to the quartet P state can proceed by the exchange of the projectile electron with the exciting target electron. Zouros et al. showed that the production cross sections was found to increase sharply with projectile energy above .75 MeV/u. Figure 9 shows data from O^{5+} on He, H_2 collisions. The energy dependence (but not the magnitude) of the thresholdlike behavior of the measured cross sections is thus found to be well described using calculated cross sections[13] for electron impact ionization found in the literature, folded with the momentum distribution or Compton profile of the target electrons. This type of accounting for the target electrons' approximately "free" nature is analogous to the impulse approximation treatment of resonance transfer excitation (RTE), which relates dielectronic recombination, another free electron-ion collision process, to that of RTE occurring in ion-atom collisions.

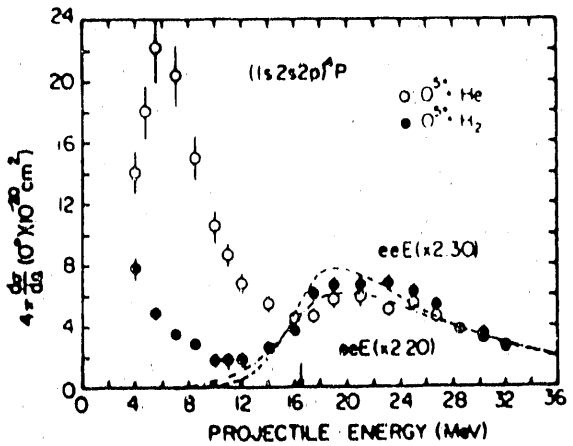

Fig. 9. Cross sections for the production of $1s2s2p\,^4P$ states by $1s \rightarrow 2p$ projectile excitation in collisions of O^{5+} with He and H_2 targets vs projectile energy. Dashed and dashed-dotted lines give corresponding scaled theoretical excitation functions, using theoretical electron impact excitation cross sections folded by the Compton profile of the target. Threshold is marked by an arrow. From Ref. 13.

Electron Impact Ionization and Excitation in Crystal Channels

Collisions between ions and the electrons of a macroscopic "molecule", namely a perfect single crystal, have long been studied in channeling experiments, where most of the interaction occurs with crystal electrons in regions distant from lattice sites, with the projectile ions colliding only gently with those of the lattice. The nearly free electrons

found near the centers of channels, spread in energy only by the Fermi distributions of the conduction or valence electrons, has been exploited by Claytor et al.[14] to determine the electron impact ionization cross sections for Be-like to H-like uranium for 222 keV electrons (in the rest frame of the projectile ions). The large density of electrons – $\gtrsim 10^{23}$ per cm^3 – makes possible the measurement of very small cross sections. In these experiments, 405 MeV/u uranium ions were channeled in the $< 110 >$ channel of Si to obtain cross sections of 3.9; 11.0; 16.0, and 31.0 b (+100%, - 50%), respectively, for $1s$, $1s^2$, $2s$, and $2s^2$ electrons. The results for the $1s$ and $1s^2$ cross sections disagree with present theory.(See Table I.)

TABLE I. Electron impact ionization cross sections (b).

Ion	State	Expt.	Pindzola&Buie	Scofield	Younger	Lotz
U^{91+}	$1s$	3.9		1.5	0.8	0.7
U^{90+}	$1s^2$	11.0		3.0	1.7	1.4
U^{89+}-U^{90+}	$2s$	16.0	13.0	29.0	9.4	12.0
U^{88+}-U^{90+}	$2s^2$	31.0	26.0	57.0	19.8	24.0

For original theoretical papers, see Ref. 14.

Resonant Coherent Excitation of Convoy Electrons in Crystal Channels

An axially channeled ion feels the anharmonic periodic potential of the crystal as an oscillatory electric field with a fundamental frequency $\nu = v/d$, where d is the atomic spacing and v the ion velocity. When the frequency (or a higher harmonic) coincides with an excitation energy of the ion, RCE can occur. This effect was first observed through the change in the charge state distribution of emergent ions[15], reflecting the higher probability for electron loss from resonantly excited states of projectile ions. Recently, Iwata et al[15] have observed photons emitted from excited states formed by RCE.

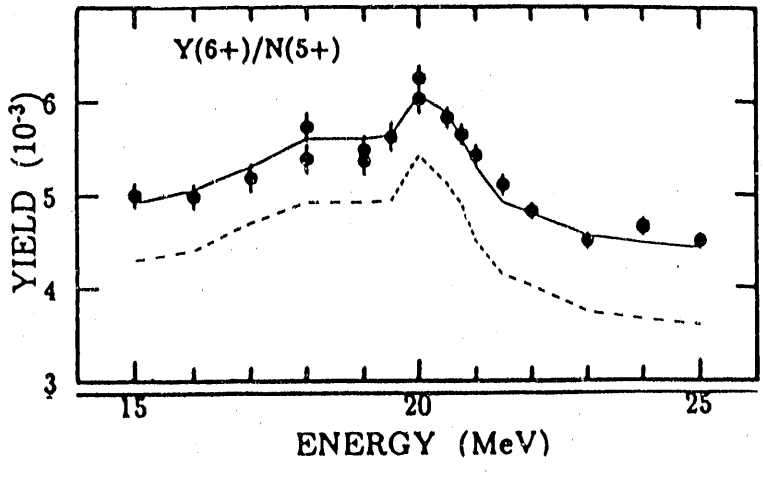

Fig. 10. Beam energy dependence of absolute convoy electron yields measured in coincidence with exit C^{6+} ions, normalized to the number of exit C^{5+} ions. The solid line shows results of a model calculation for ELC, and the dashed line shows the calculated contribution from excited states. From Ref. 16.

Very recently, Kimura et al.[16] have made the first identification of a clear effect of RCE on convoy electron production. Figure 10 shows a large enhancement of the yield of convoy electrons in coincidence with C^{6+} ions traversing the ⟨100⟩ axis of 160 nm thick Au crystals, normalized to the number of exit C^{5+} ions, as the incident velocity is swept through the second harmonic $1s-2s$ and $2p$ (RCE) resonances near 20 MeV. A detailed rate-equation production model fit to the data, which includes separate treatment of the C^{5+} ground and excited state populations, reveals that while the fraction of all C^{5+} ion in the excited state is $\lesssim 1/3$, these excited ions contribute to $\gtrsim 80\%$ of the convoy yield!

Dielectronic Excitation and Recombination – in Crystal Channels and in Resonant Transfer Excitation

Strictly speaking, dielectronic recombination is a resonant process in which a free electron of carefully selected relative velocity resonantly excites a bound target electron to an excited state, sticks to form a doubly excited state, and radiative stabilization of the recombined atom or ion then occurs. Though it is tempting and timely to discuss the beautifully resolved dielectronic recombination resonances observed in the recent work of Andersen et al.[17], we elect to bypass this interesting subject because it has been so extensively discussed and reviewed in many recent conferences and review articles, because it focusses primarily on free electron-ion collisions, and also because it is to discussed by others (e.g., Tanis and Cocke) in subsequent papers at this Workshop.

In a series of recent experiments, Datz et al.[18] have succeeded in studying dielectronic excitation and recombination in crystal channels. These phenomena were observed for H-like S, Ca, and Ti, and for He-like Ti, traversing the $<110>$ and $<100>$ channels in Si. Sample data is shown in Fig. 11, which exhibits for Ca^{19+} the yield per injected ion of unresolved $h\nu_1(2\ell n\ell' \rightarrow 1sn\ell')$ plus $h\nu_3(2\ell \rightarrow 1s)$ transitions. Both arise from filling a K hole in an empty K shell. The features correspond to dielectronic excitation of KLL, KLM, KLN, etc., and, at 300 MeV, to $1s \rightarrow 2p$ excitation. The dielectronic recombination resonances are broadened and reduced in amplitude, owing to the small but finite width of the electron Fermi energy distribution (≈ 10 eV).

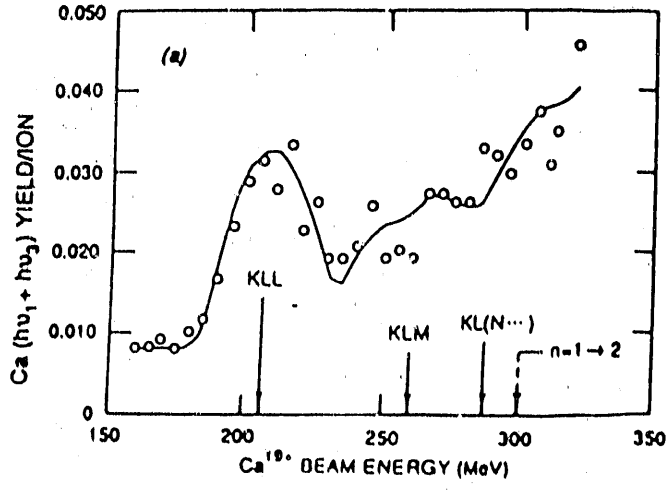

Fig. 11. Yield of $h\nu_1(2\ell n\ell' \rightarrow 1sn\ell')$ plus $h\nu_3(2\ell \rightarrow 1s)$ as a function of Ca^{19+} ion energy incident on a $<110>$ channel in a 1.2 μm thick Si crystal. Thresholds for various dielectronic processes are shown. The solid curve corresponds to a computer simulation. From Ref. 18.

That similar phenomena occur in ion-atom collisions, where electron transfer from a target atom is accompanied by simultaneous excitation of a bound projectile electron, has been known for quite some time. Tanis has recently provided two reviews[19]. In this case resonances are broadened more strongly still than for dielectronic recombination of ions in crystals, owing to the folding of the bound electrons' momentum distribution (Compton profile) with the resonances.

Because Tanis is to discuss this subject subsequently in this Workshop, no doubt more expertly than I, it seems best to leave the bulk of discussion about resonant transfer and excitation (RTE) to him. Here we provide only two illustrations of the transfer excitation process. The first is Fig. 12, which presents a schematic overview of the three different known mechanisms which lead to transfer excitation in energetic ion- atom collisions – the resonant mechanism just discussed, in which electron-electron interactions between projectile and target electrons dominate; non-resonant transfer excitation (NTE), which occurs through independent capture by the projectile coincident with projectile electron excitation by the target nucleus; and the so-called uncorrelated transfer excitation (UTE), coming from target electron excitation of a projectile electron, coincident with electron capture by the projectile. In the systems so far investigated, the NTE and UTE processes tend to dominate the TE probability at somewhat lower and higher projectile energies, respectively, than the range for which RTE dominates.

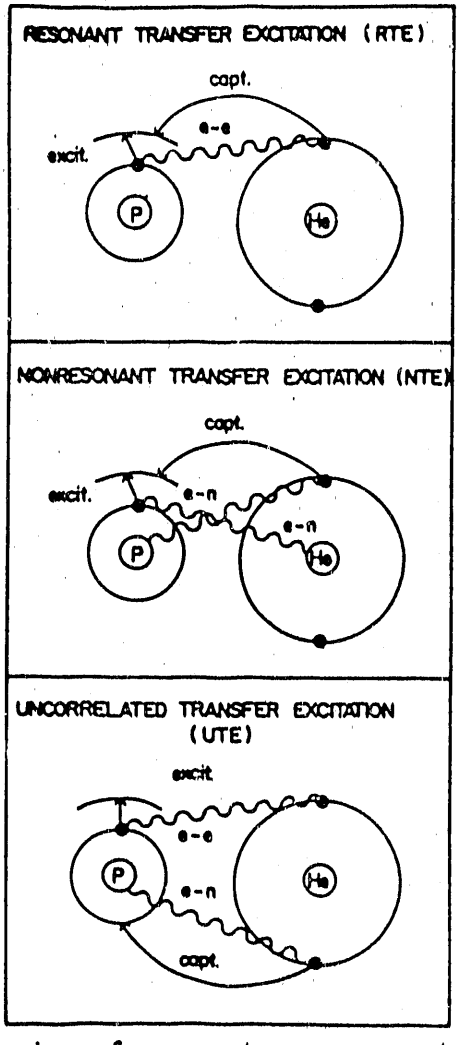

Fig. 12. Schematic overview of resonant, nonresonant, and uncorrelated transfer excitation processes. From J. A. Tanis, presented at the U. S.- Japan Seminar on Exotic and Highly Ionized Ions, Anchorage, June, 1990.

This situation is illustrated in Fig. 13, which shows the various contributions to TE for S^{13+} on He, observed in the x-ray decay channel.

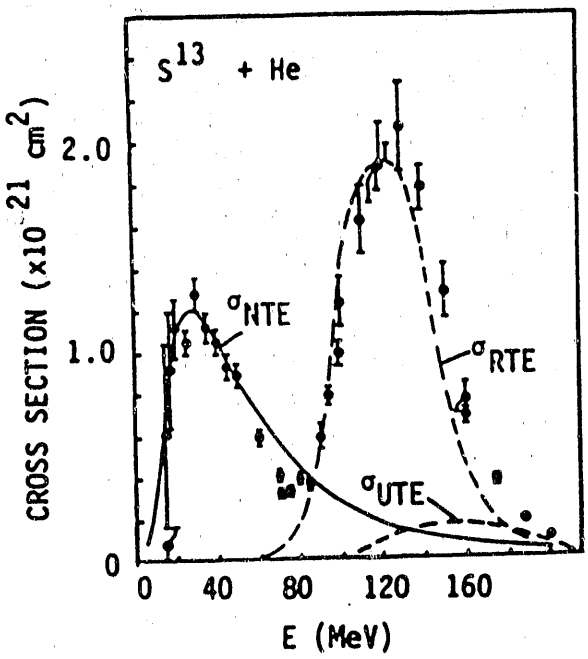

Fig. 13. Transfer excitation cross sections for S^{13+} on He. Data measured by J. Tanis et al. [Phys. Rev. A31, 4040 (1985)] are for S K x-rays coincident with single capture. The upper dashed curve is the calculated RTE cross section X 0.85, and the solid curve is the calculated NTE cross section normalized to the data. The lower dashed curve is the estimated UTE cross section taken from the work of Y. Hahn and H. Ramadan, Nucl. Inst. Meth. B43, 285 (1989). From Ref. 19.

Similarity of Recoil Ion Spectra Observed in Coincidence with Electron Capture vs. Electron Loss

In a paper by Levin et al.[20] concerning the decisive importance of vacancy cascades in determining high recoil ion charge state distributions in nearly symmetric, 0.7 MeV/u Cl on Ar collisions, the recoil ion charge state spectrum was studied in coincidence with single and double, electron capture and loss collisions. The remarkable similarity of the recoil ion spectra for coincident double capture vs. double loss is apparent in Fig. 14.

The enrichment of highly ionized states in the recoil spectrum corresponding to capture of two L-shell electrons proved easy to explain quantitatively by considering the additional autoionization corresponding to two vacancy cascades. The nearly identical appearance of the recoil spectra coincident with double electron loss strongly suggests that loss of two projectile L-shell electrons is highly correlated with ionization of two L-shell target electrons in the same collision. (Similar results were obtained in comparing recoil ion spectra for single capture and loss). Electron-electron collisions among target and projectile electrons giving rise to symmetric ionization of both is a plausible mechanism for accounting for this mutual ionization. Although the fast collision conditions prevailing are well out of the adiabatic collision regime for which molecular orbital collision models are expected to apply, such a mechanism is reminiscent of the promotion of $4f\sigma$MO's into the continuum, well known to produce L-shell vacancies in much lower energy collisions.

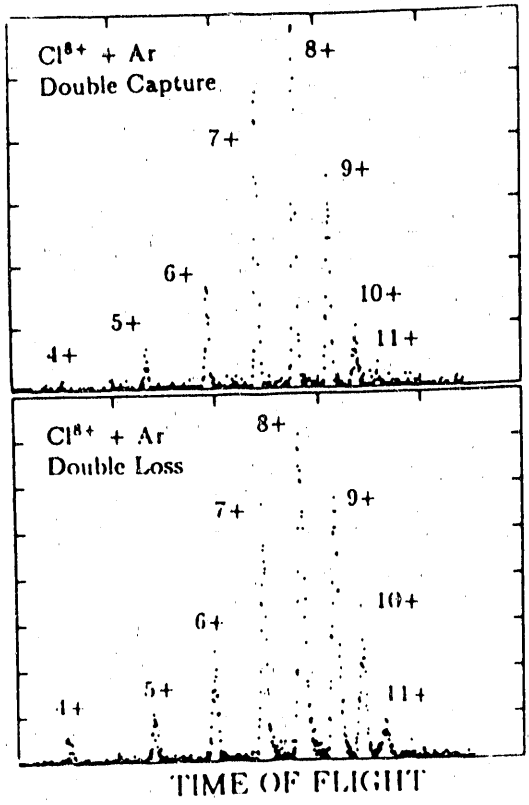

Fig. 14. Time of flight spectra for Ar recoil ions produced by beams of 0.7 MeV/u Cl ions, measured in coincidence with double electron capture, and double electron loss, respectively. Note the remarkable similarity of the recoil ion spectra for double capture vs. double loss. From Ref. 20.

New Research on Ion-Atom Collisions Physics at Relativistic Energies

We conclude with some examples of new experiments in which the role of electrons – and in this case, their positron antiparticles – is again decisive, but in the domain of relativistic atomic collisions. In our choice of examples we draw upon the work of a panel that considered relativistic atomic collisions within a larger workshop on future opportunities in atomic and molecular science held in 1989.[21]

The first of two main areas of research identified as having high potential by the panel lies in the area of fast heavy ion-atom collisions: Because peripheral atomic collisions at TeV/u energies can be viewed as virtual photon-photon collisions owing to Lorentz contraction of the Coulomb fields, the resultant production of single and multiple electron-positron pairs presents new experimental and theoretical challenges. For example, in TeV/u U + U collisions, the projectile field at a target nucleus appears essentially as an intense pulse of photons with energies $\gtrsim$ 100 GeV, not only permitting copious production of electron-positron pairs but also elementary particle pairs (muons, tauons, W's, etc.). While possibilities for studying such collisions do not yet exist, beams of 1 GeV/u U presently exist at GSI and LBL, and of 200 GeV/u S at CERN.

Examples of particular experimental possibilities include:

(1) Study of the differential cross section for electron-positron pair production, including the energy and angular distribution of both electrons and positrons. There seems to be a wide variation in theoretical predictions for these cross sections[21];

(2) Pair production with capture of the electron into a vacant projectile (K) shell. Experimentally, this process can be distinguished from free pair production because of the charge change of the projectile. Though the cross section is thought to be an order

of magnitude or two smaller than that for free pair production, it is also thought to be measurable already at a relativistic time dilation factor $\gamma = 2$;

(3) Radiative electron capture accompanied by electron-positron pair emission. For fast enough collisions, it has long been known that electron capture from a target atom accompanied by photon emission can dominate over mechanical capture. Preliminary calculations[21] indicate that for $\gamma \gtrsim 3$, radiative capture accompanied by electron-positron pair emission may be detectable. If so, a careful discrimination between possibilities (2) and (3) must be made, since in the former charge state change occurs with positron emission alone, while in the latter a pair is emitted.

At the time of writing an initial experiment[22] set up to explore possibilities (1) and (2) is underway at the CERN SPS facility. The experiment is being run with 200 GeV/u S beams on Au, and (for testing scaling and calibration), Al and Pd. Recent calculations by Rhoades-Brown, Bottcher, and Strayer[22] for the cross sections for capture for various symmetric pairs are shown in Fig. 15.

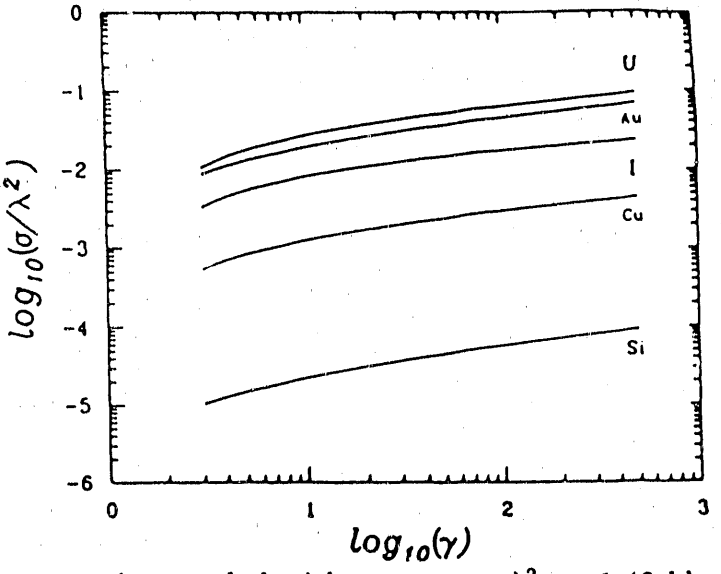

Fig. 15. Capture cross sections scaled with respect to $\lambda^2 = 1.49$ kb, where λ is the rationalized Compton wave length, for the various symmetric collision pairs marked. From Ref. 22.

If the cross section is scaled as Z^2, the cross section for the S on Au collision system at the γ value corresponding to the available center of mass energy is predicted to be $\approx$ 2b.

Work supported in part by the National Science Foundation and by the U.S. Department of Energy, Office of Basic Energy Sciences, Division of Chemical Sciences, under Contract No. DE-AC05-840R21400 with Martin Marietta Energy Systems, Inc.

References

1. J. C. Levin, C. Biedermann, N. Keller, L. Liljeby, C.-S. O, R. T. Short, and I. A. Sellin, Phys. Rev. Lett. 65, 988 (1990).
2. Z. Smit, M. Kregar, and D. Glavic-Cindro, Phys. Rev. A 40, 6303 (1989).
3. L. H. Andersen, P. Hvelplund, H. Knudsen, S. P. Møller, K. Elsener, K.-G. Rensfelt, and E. Uggerhøg, Phys. Rev. Lett. 57, 2147 (1986). For a very recent discussion of shakeoff and the so-called TS-1 process, see the paper of L. Végh and J. Burgdörfer, Phys. Rev. A42, 655 (1990).

4. J. F. Reading and A. L. Ford, Phys. Rev. Lett. 58, 543 (1987); J. Phys. B21, L685 (1988).

5. O. Heber, B. Bandong, G. Sampoli, and R. L. Watson, Phys. Rev. Lett. 64, 851 (1990).

6. J. McGuire, private communication; Phys. Rev. Lett. 49, 1153 (1982); Nucl. Inst. Meth. B 10/11, 17 (1985).

7. M. Charlton, L. H. Andersen, L. Brun-Nielsen, B. I. Deutsch, P. Hvelplund, F. M. Jacobsen, H. Knudsen, G. Larrichia, M. R. Poulsen, and J. O. Pedersen, J. Phys. B21, L545 (1988).

8. J. Pálinkás, R. Schuch, H. Cederquist, and O. Gustafsson, Phys. Rev. Lett. 63, 2464 (1989); J. Briggs and K. Taulbjerg, J. Phys. B 12, 2569 (1979).

9. J. Giese, M Schulz, J. Swenson, H. Schöne, M. Benhenni, S. Varghes, C. Vane, P. Dittner, S. Shafroth, and S. Datz, to be published in Phys. Rev. A; corrected data of J. O. P. Pedersen and P. Hvelplund, Phys. Rev. Lett. 62, 2373 (1989); W. Fritsch and C. D. Lin, to be published in Phys. Rev. A.

10. O. Heil, A. Kövér, G. Szabó, L. Gulyás, K. Tökési, J. Kemmler, H. Rothard, D. Berényi, and K. O. Groeneveld, Inst. für Kernforschung der Uni. Frankfurt/M Annual Report No. IKF-47, p. 19 (1987), and J. Phys. B 21, 3231 (1988); H. Hartley and H. Walters, J. Phys. B 20, 3811 (1987); J. Wang and J. Burgdörfer, private communication, and to be published.

11. J. Burgdörfer et al., Phys. Rev. Lett. 51, 374 (1983); J. Burgdörfer, M. Breinig, S. B. Elston, and I. A. Sellin, Phys Rev. A 28, 3277 (1983); L. Gulyás, A. Kövér, G. Szabó, D. Berényi, L. Sarkadi, J. Pálinkás, and T. Vajnai, "Cusp Inversion in the Electron Loss Process", ECAMP - 3, Bordeaux, 1989; J. Burgdörfer and G. Szábo, to be published.

12. H.-P. Hülskötter, W. E. Meyerhof, E. Dillard, and N. Guardala, Phys. Rev. Letters 63, 1938 (1989).

13. T. J. M. Zourcs, D. H. Lee, and P. Richard, Phys. Rev. Lett. 62, 2261 (1989); S. J. Goett and D. H. Sampson, At. Data Nucl. Data Tables 29, 535 (1983).

14. N. Claytor, B. Feinberg, H. Gould, C. Bemis, J. Gomez del Campo, C. Ludemann, and C. R. Vane, Phys. Rev. Letters 61, 2081 (1988).

15. S. Datz, C.D. Moak, O.H. Crawford, H.F. Krause, P.F. Dittner, J. Gomez del Campo, J.A. Biggerstaff, P.D. Miller, P. Hvelplund, and H. Knudsen, Phys. Rev. Lett. 40, 843 (1978); Y. Iwata, K. Komaki, Y. Yamazaki, M. Sekiguchi, T. Hattori, T. Hasegawa and F. Fujimoto, Nucl. Inst. Meth. B48, 163 (1990).

16. K. Kimura, J. Gibbons, S. Elston, C. Biedermann, R. DeSerio, N. Keller, J. Levin, M. Breinig, J. Burgdörfer, and I. Sellin, submitted for publication.

17. L. Andersen, P. Hvelplund, H. Knudsen, and P. Kvistgaard, Phys. Rev. Lett. 62, 2656 (1989).

18. S. Datz, C. Vane, P. Dittner, J. Giese, J. Gomez del Campo, N. Jones, H. Krause, P. Miller, M. Schulz, H. Schöne, and T. Rosseel, Nucl. Inst. Meth. B48, 114 (1990).

19. See for example the excellent reviews by J. A. Tanis, "Electron Transfer and Projectile Excitation in Single Collisions", Nucl. Inst. Meth. A262, 52 (1987); and in the Proceedings of the X-90 International Conference on X-rays and Inner Shell Ionization, to be published in Nucl. Inst. Meth.

20. J. Levin, C.-S. O, H. Cederquist, C. Biedermann, and I. Sellin, Rapid Communications, Phys Rev. A38, 2674 (1988).

21. Report of the Panel on Relativistic Atomic Collisions, Future Opportunities in Atomic, Molecular, and Optical Sciences Workshop, November 7, 1989. Panel members: C. Bottcher, H. Bryant, H. Gould, W. Meyerhof, P. Mohr, and W. Smith. See also R. Anholt and H. Gould, in Advances in Atomic and Molecular Physics, D. Bates and B. Bederson, eds., (Academic Press, New York, 1986) Vol. 22, p. 315.

22. Participants include S. Datz, C. Vane, P. Dittner, H. Gould, H. Knudsen, P. Hvelplund, R. Schuch et al. The theoretical calculations displayed in Fig. 15 are from M. J. Rhoades-Brown, C. Bottcher, and M. Strayer, Physical Review A 40, 2831 (1989), and Nucl. Inst. and Meth. B43, 301 (1989).

END

DATE FILMED

10 / 23 / 90